

pH Study and Partition of Riboflavin in an Ethyl Lactate-Based Aqueous Two-Phase System with Sodium Citrate

Pedro Velho Ines Oliveira Elena Gómez and Eugénia A. Macedo

Cite This: *J Chem Eng Data* 2022 67 1985–1993

Read Online

ACCESS |



Metrics & More

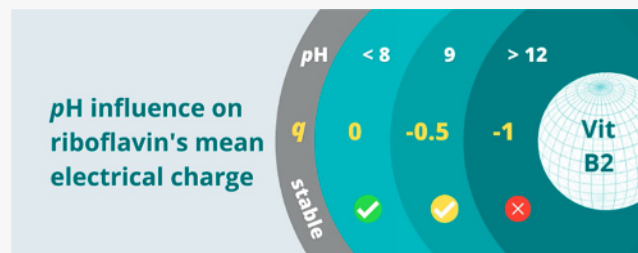


Article Recommendations



Supporting Information

ABSTRACT: Antioxidants neutralize reactive oxygen species in excess in animal bodies, ensuring a proper reduced state of the cells and avoiding the appearance of diseases. Since antioxidants are very reactive, they are heavily affected by changes in pH, which may influence partition and hamper solute quantification due to chemical structure and conformation modification. Natural antioxidants are present, for example, in fruit pomaces, and could be extracted for food supplementing purposes, contributing to a more circular economy. Aqueous Two-Phase Systems (ATPS) constitute a liquid–liquid extraction technique which has been applied with success in the recovery of bioproducts due to its sustainability and biocompatibility. Ethyl lactate and organic salts-based ATPS are considered very eco-friendly because of their high biodegradability and low toxicity. In this work, the extraction of riboflavin (vitamin B2) was successfully performed in the ATPS {ethyl lactate (1) + sodium citrate (2) + water (3)} at 298.15 K and 0.1 MPa. This was accomplished after a careful study of the influence of pH in the UV–vis spectra and allowed to obtain a maximum partition coefficient (K) of 6.61 and a maximum extraction efficiency (E) of 87.6 for the longest tie-line (TLL = 69.68) with antioxidant losses below 3 .



1. INTRODUCTION

The purification and recovery of biomaterials such as proteins, antibodies, and enzymes cannot be performed at high temperatures and pressures nor by using solvents which could damage the solutes by causing denaturation and loss of the labile biomolecules,¹ so high water-content and low ionic strength systems are required.²

Aqueous Two-Phase Systems (ATPS), a liquid–liquid fractionation technique, had a surge in the recovery of bioproducts³ mostly because of its cost-effectivity, sustainability, simplicity, versatility, biocompatibility, scalability, and high extraction yield.^{3–5} However, they are still regarded as a primary recovery stage due to their low selectivity,⁵ which has been enhanced by properly choosing the ATPS-forming chemical compounds, adjusting ionic strength, and adding biospecific affinity ligands.^{2,3,6} Besides the electrochemical potential and bioaffinity, phase hydrophobicity and the solute's molecular size and chemical conformation are thought to heavily influence the phases' selectivity for biomolecules.⁷

The most common ATPS include two polymers (e.g., polyethylene glycol/dextran⁸), a polymer and a salt (e.g., PEG/ammonium sulfate⁹), a polymer and a low molecular weight alcohol (e.g., PEG/ethanol¹⁰), an ionic liquid and a salt (e.g., [Amim][Cl] and potassium carbonate¹¹), or a low molecular weight alcohol and a salt (e.g., ethanol/potassium phosphate¹²). Generally, polymer-based ATPS present lower ionic strength than salt-based ATPS but are very expensive and lead to a slow segregation of the phases. On the other hand,

alcohol-based ATPS are a very cheap technology, but most proteins and enzymes are not compatible with an alcohol-rich phase.^{2,12}

ATPS based on green organic solvents and on a salt have extensively been used in the extraction of amino acids, proteins, antioxidants, and other natural products, because they do not present any threat to the environment and they preserve the bioactivity of the solutes.¹² In these ATPS, the salt is the responsible for promoting phase separation (it is the salting-out agent) and the most environmentally friendly options are organic salts, such as citrates and tartrates, since they are biodegraded without damage to the ecosystems.¹³ Concerning green organic solvents, ethyl lactate, the ethyl ester of lactic acid, is an eco-friendly solvent (with low toxicity and high biodegradability) with an effectiveness comparable to oil-based solvents¹⁴ and can be produced from fermenting biomass raw materials.^{13–16}

The conversion of biomass and industrial waste, which are continuously being replenished, to useful chemicals (as high added-value compounds) is a must for reducing the environ-

Special Issue: In Honor of Joan F. Brennecke

Received: November 30, 2021

Accepted: February 10, 2022

Published: February 18, 2022



Table 1. Chemicals Used with Respective Commercial Suppliers, Purities, Chemical Abstracts Service (CAS) Number, and Abbreviation

chemical	supplier	purity ^a /wt % ^b	CAS	abbreviation
acetic acid (CH ₃ COOH)	Merck	>99.8	64-19-7	
ethanol (CH ₃ CH ₂ OH)	Sigma-Aldrich	>99	64-17-5	
sodium hydroxide (NaOH)	Merck	>99	1310-73-2	
sodium citrate tribasic dehydrate (C ₆ H ₅ Na ₃ O ₇ ·2H ₂ O)	Sigma-Aldrich	>99	6132-04-3	Nacitrate
purified water (H ₂ O)	VWR chemicals		7732-18-5	
(–) ethyl L-lactate (C ₅ H ₁₀ O ₃)	Sigma-Aldrich	>98	97-64-3	EL
riboflavin (C ₁₇ H ₂₀ N ₄ O ₆)	Sigma-Aldrich	>99	83-88-5	B2

^aProvided by the supplier. ^bwt % refers to weight percentage.

mental impact of human activity and ensuring a more circular economy.¹⁷ Natural antioxidants are present in common wastes, such as woody biomass,¹⁸ olive mill wastewater,¹⁹ and fruit pomaces²⁰ and could be extracted for food supplementing purposes.

Antioxidants stabilize the reactive oxygen species (ROS) in excess in animal bodies, acting as redox couples and ensuring a proper reduced state of the cells.²¹ They have a preponderant role in, for example, preventing eye cataracts,²² enhancing animal immune systems,²³ conserving mammalian semen,²⁴ and avoiding premature aging.²⁵

Riboflavin, or vitamin B2, is a water-soluble antioxidant with a recommended human daily intake of 1.3 mg for adolescents and adults which is naturally present in eggs, meat, vegetables, and legumes.²⁶ In underdeveloped countries, ensuring the minimum consumption may be hard, and its deficiency is linked to neurological disorders, inflammation of the lips (cheilosis), skin problems (seborrheic dermatitis), and anemia.²⁶ This vitamin has been successfully separated using ATPS with PEG and organic salts (sodium citrate and sodium tartrate),²⁷ but the obtained partition coefficients were rather low ($K < 3.5$) and the separation of the solute from the polymer is hard to perform without damaging the biomolecule.

Since antioxidants are very labile species, they are very sensitive to changes in pH, which may affect partition and even hamper solute quantification due to chemical structure and conformation modification. The main goal of this work was to perform the extraction of riboflavin (B2) in the ATPS {ethyl lactate (1) + sodium citrate (2) + water (3)} at 298.15 K and 0.1 MPa with a thorough study of the influence of pH in the UV–vis spectra for future application in the recovery of riboflavin from biowastes such as fruit pomaces and vegetable peels.

2. EXPERIMENTAL METHODS

2.1. Chemicals and Apparatus. The chemicals used and their respective supplier, purity, CAS number, and abbreviation can be seen in Table 1. All of them were used without further purification steps.

Concerning the apparatus used, mass (m) was determined with a OHAUS Pioneer PA214C balance with measurement uncertainty of $\pm 1 \times 10^{-4}$ g. pH was determined with a VWR pH 1100 L pH meter with uncertainties of ± 0.001 in the measurement of pH and ± 0.1 K in the measurement of temperature. Temperature (T) was kept at 298.15 K with an OVAN Therm H TH100E thermostatic bath coupled with a magnetic stirrer with an uncertainty of ± 0.01 K. Density (ρ) was determined with an Anton Paar DSA-5000 M densimeter, which has an uncertainty of $\pm 3 \times 10^{-5}$ g·cm⁻³ in density and 0.01 K in temperature. Liquid volumes (V) were measured

with an Eppendorf Multipipette E3x electronic pipet with an uncertainty of 0.5 L when using the 200 L tips. Absorbance was measured with a Thermo Scientific Varioskan Flash UV–vis spectrophotometer with an uncertainty of 10^{-4} in absorbance. Samples were stirred with a VWR vortex VV3 and with an IKA RO 10 P magnetic stirrer.

2.2. Influence of pH in the Absorbance Spectrum.

Five stock solutions of riboflavin in water were prepared close to maximum solubility at 298.15 K (concentrations were about 8×10^{-5} g·mL⁻¹). When needed, the pH of the solutions was adjusted from the initial value of 6.6 by consecutively adding drops of 0.5 M aqueous solutions of sodium hydroxide (NaOH) or acetic acid (CH₃COOH) and mixing for 3 min in a IKA RO 10 P magnetic stirrer, obtaining pH = 3.3, 6.5, 8.1, 9.7, and 12.3. These values were determined with a VWR pH 1100 L pHmeter. The masses of added NaOH and CH₃COOH were measured using the OHAUS Pioneer PA214C balance and the antioxidant concentrations were recalculated having this in consideration. Using an Eppendorf Multipipette E3x electronic pipet, 200 L samples of each stock solution were taken and added to a Greiner bio-one polystyrene flat bottom plate with 96 wells. Then, an absorbance screening was performed from 200 to 600 nm with the Thermo Scientific Varioskan Flash UV–vis spectrophotometer with the samples previously stabilized at 298.15 K.

2.3. Influence of pH in the Absorbance Spectrum Stability.

The five stock solutions prepared earlier were left to settle for 3 days at 298.15 K without any special protection from daylight. Then, 200 L samples of each stock solution were added to a Greiner bio-one polystyrene flat bottom plate with 96 wells and a new absorbance screening was carried out with the Thermo Scientific Varioskan Flash UV–vis spectrophotometer from 200 to 600 nm with previously stabilized samples at 298.15 K. These spectra were compared with those previously obtained.

2.4. Absorbance Calibration Curve. Twelve mixtures with different concentrations of antioxidant and with a total volume of 2 mL were prepared in 3 mL vials by diluting the stock solution (8.37×10^{-5} g·mL⁻¹, pH = 8.1) prepared earlier in the day. After preparation, the vials were capped and sealed with parafilm, and then the mixtures were vigorously stirred in a VWR VV3 vortex for about 1 min and in an IKA RO 10 P magnetic stirrer for 10 min. Afterward, 200 L samples of each vial were added to a Greiner bio-one polystyrene flat bottom plate with 96 wells and a new absorbance screening was carried out with the Thermo Scientific Varioskan Flash UV–vis spectrophotometer from 200 to 600 nm with previous stabilization at 298.15 K. Then, a calibration curve was prepared by plotting the antioxidant concentrations and the

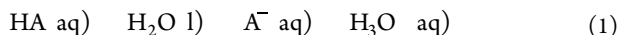
respective absorbances at the chosen wavelength and fitting the experimental points to a first-degree equation. The absorbance of water (and plate) was subtracted from the curve points.

2.5. Partitioning of Biomolecules. Six mixtures of 10 mL were prepared in different numbered vials corresponding to six well-known tie-line compositions of the ATPS {ethyl lactate (1) + sodium citrate (2) + water (3)} by pipetting and weighing the pure compounds (water and ethyl lactate) and a previously prepared aqueous solution of sodium citrate salt (26.07 wt %). To maintain the tie-lines compositions, it is important to refer that 1 mL of pure water was substituted by 1 mL of the stock solution of the antioxidant (8.37×10^{-5} g·mL⁻¹, pH = 8.1). Next, the vials were capped and sealed with parafilm and vigorously agitated in the vortex for 1 min and left in the OVAN Therm H TH100E thermostatic bath coupled with a magnetic stirrer for 6 h at 298.15 K and 0.1 MPa. After stirring, the vials were left settling overnight, which corresponds to approximately 12 h, at the same temperature. Then, the top and bottom phases were carefully removed using syringes and weighed in the OHAUS Pioneer PA214C balance. The absorbances of the two phases of all the mixtures were determined following the methodology described above and the pHs were measured with the VWR pH 1100 L pH meter. Finally, phase densities were measured with an Anton Paar DSA-5000 M densimeter and the instrument was cleaned between measurements first with water and last with ethanol.

3. RESULTS AND DISCUSSION

3.1. Influence of pH in the Absorbance Spectrum. At specific pH values, the acid dissociation of antioxidants changes the chemical structure and chemical conformation of these biomolecules and can affect the absorbance spectra, which hampers the experimental determination of their concentration. Therefore, in this section, the influence of pH on the absorbance spectra of riboflavin (B2) was studied. This evaluation will be essential to understand whether this ATPS is suitable for extracting riboflavin without affecting its structure and whether the pH of the stock solution used in the calibration curve has to match the pH of partition.

Riboflavin (vitamin B2) has a pK_a of 9.69 at 298.15 K.²⁸ Acetic acid, for example, has a pK_a of 4.76 at the same temperature, so riboflavin is a significantly weaker acid. The equilibrium reaction in water of one acid can be written as²⁹



where HA refers to a generic acid (antioxidant) and A⁻ to its reduced species.

Depending on the number of pK_a values an antioxidant may have, it can present chemical structures with different electric charges, which will be referred to in this work as antioxidant stages. The larger the pH of a solution is, more negative the antioxidant charge becomes, which implies weaker acidic behavior of the antioxidant stages and, therefore, smaller successive acid dissociation constants.

The acid dissociation constant (K_a) of the reaction presented in eq 1, which can be written in terms of activities²⁹ or concentrations, is

$$K_a = \frac{[\text{A}^-][\text{H}_3\text{O}^+]}{[\text{HA}][\text{H}_2\text{O}]} \quad (2)$$

where [A⁻], [H₃O⁺], [HA], and [H₂O] designate the concentrations (mol/L) of the respective species in solution.

The concentration of water is generally taken as constant, so the expression can be simplified into

$$K_a = \frac{[\text{A}^-][\text{H}_3\text{O}^+]}{[\text{HA}]} \quad (3)$$

Taking the negative logarithm of both terms, comes

$$-\log K_a = -\log \left(\frac{[\text{A}^-]}{[\text{HA}]} \right) - \log [\text{H}_3\text{O}^+] \quad (4)$$

which is the same as²⁹

$$pK_a = \log \left(\frac{[\text{H}_3\text{O}^+]}{[\text{A}^-]/[\text{HA}]} \right) = \text{pH} \quad (5)$$

Since the pK_a of riboflavin is known (9.69 at 298.15 K²⁸), the ratio between its neutral and reduced stages ($[\text{HA}]/[\text{A}^-]$) can be calculated for each pH by rearranging eq 5. Afterward, the fractions of each antioxidant stage are easily calculated using eqs 6 and 7.

$$x_{\text{HA}} = \frac{[\text{HA}]}{[\text{HA}] + [\text{A}^-]} \quad (6)$$

$$x_{\text{A}^-} = \frac{[\text{A}^-]}{[\text{HA}] + [\text{A}^-]} \quad (7)$$

where x_{HA} and x_{A^-} are the fractions of riboflavin in the neutral (HA) and reduced (A⁻) antioxidant stages, respectively.

Then, the mean electrical charge of the antioxidant in aqueous solution (q) can be determined by a weighted arithmetic mean

$$q = x_{\text{HA}} q_{\text{HA}} + x_{\text{A}^-} q_{\text{A}^-} \quad (8)$$

where q_{HA} (0 e) and q_{A^-} (-1 e) are the electrical charges of the antioxidant stages HA and A⁻, respectively.

Figure 1 shows the calculation results for the riboflavin's mean electric charge (q) at different pH values. In the

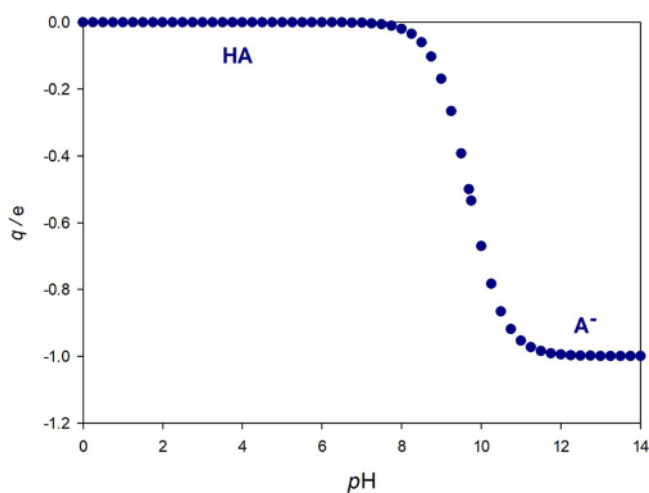


Figure 1. Influence of pH on the mean charge (q) for riboflavin.

Supporting Information, Table S1, the calculated fractions (x_{HA} and x_{A^-}) of each antioxidant stage can be seen for the points shown in Figure 1.

As it can be seen in Figure 1, q is significantly affected with pH, and different charges can coexist at the same pH, which may affect the absorbance spectrum. As expected, when pH corresponded to the value of riboflavin's pK_a (9.69), there was

an equal fraction of the two antioxidant stages ($x_{\text{HA}} = x_{\text{A}^-}$), as can be seen in Table S1, in the [Supporting Information](#).

In previous works,¹³ the pH of the obtained ternary phases in the APTS {ethyl lactate (1) + sodium citrate (2) + water (3)} was approximately equal to 7 in both phases. Hence, from [Figure 1](#), it can be seen that this system is appropriate to extract the neutral stage of riboflavin. However, it is still needed to study how the different antioxidant stages present affect the absorbance spectra, so solutions of riboflavin with different pH values (3.3, 6.5, 8.1, 9.7, and 12.3) were prepared and an absorbance screening was carried out from 200 to 600 nm, as [Figure 2](#) shows.

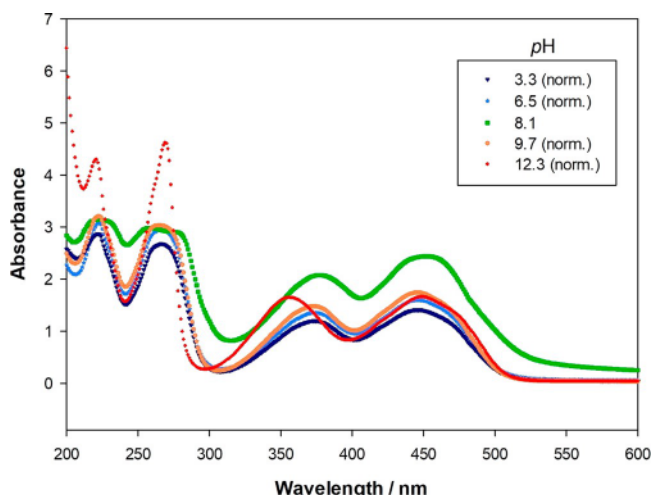


Figure 2. Influence of pH in the absorbance spectra of riboflavin.

In [Figure 2](#), the absorbances of the solutions at pH = 3.3, 6.5, 9.7, and 12.3 were normalized to allow for proper comparison using the equation

$$\bar{A} = \frac{C_{\text{ref}}}{C_i} \quad (9)$$

where \bar{A} is the normalized absorbance, A is the experimental absorbance, C_{ref} is the reference concentration ($8.37 \times 10^{-5} \text{ g} \cdot \text{mL}^{-1}$, pH = 8.1) and C_i is the concentration of the solution under normalization. The measured absorbances can be observed in the [Supporting Information](#), Table S2.

As it can be seen in [Figure 2](#), the absorbances generally increase from pH = 3.3 to pH = 8 in the entire wavelength range. However, in higher pH values (9.7 and 12.3), this trend only holds in wavelengths below 300 nm. For that reason, in this region the absorbance of the system is less sensitive to changes in the pH and should be preferred in the determination of the calibration curve. Above the value of 300 nm, the absorbance of riboflavin is generally lower at larger pH values. All of this shows that the existence of differently charged antioxidant stages of riboflavin significantly interferes with absorbance and that spectra are a result of the contribution of all the different antioxidant stages which may coexist. At pH values lower than 9.69, the spectra behavior corresponds mostly to the neutral species ($x_{\text{HA}} > x_{\text{A}^-}$) and above that pH value the dominant spectra belong to the negative species ($x_{\text{HA}} < x_{\text{A}^-}$).

Finally, since pH turned out to be a decisive factor for the absorbance spectra, the absorbances calibration curve should

be determined at the pH of the partitioning so as to accurately quantify riboflavin.

3.2. Influence of pH in the Preservation of the Absorbance Spectrum. The presence of charged stages of the antioxidant increases the reactivity of the solutions, which may see their absorbance spectra affected after having reacted with species such as oxygen or by undergoing photo-degradation. Because of this reactivity and since partition experiments for this antioxidant take more than 18 h, it is necessary to ensure that the absorbance spectrum has not changed during the process and that it corresponds to the one used for the calibration curve. Therefore, the previously prepared riboflavin's solutions with different pH values (3.3, 6.5, 8.1, 9.7 and 12.3) were left to settle for about 3 days and the spectra were compared to those obtained initially.

From [Figure 3](#), it is noticeable that the absorbance spectrum of riboflavin remained stable even after 3 days at pH = 8.1. The

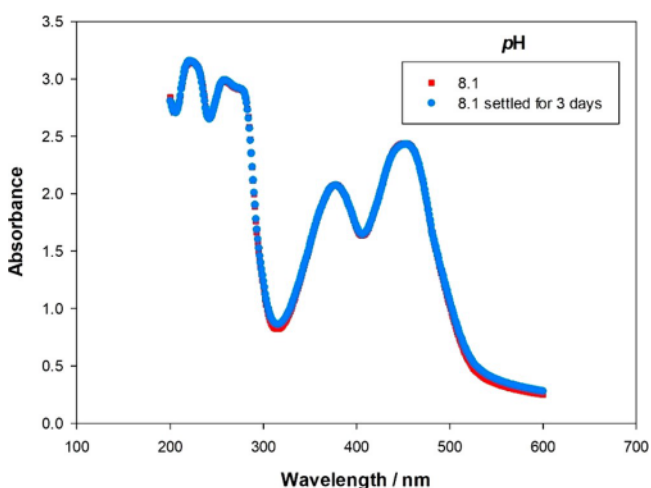


Figure 3. Influence of 3 days of settling on the absorbance spectrum of $8.4 \times 10^{-5} \text{ g} \cdot \text{mL}^{-1}$ of riboflavin in water at pH = 8.1, 298.15 K and 0.1 MPa.

same result was obtained for the solutions at pH = 3.3, 6.5, as [Figures S5 and S6](#), respectively, show in the [Supporting Information](#).

For the solution at pH = 12.3, a significant variation of the absorbance spectrum was observed after 3 days, as [Figure 4](#) demonstrates. Moreover, at pH = 9.7 some instability was noticed, as can be observed in [Figure S7](#) in [Supporting Information](#).

From [Figures 4 and S6](#) and [Table S1](#), it can be concluded that the increasing fraction of the antioxidant stage with $q = -1$ e (A^-) leads to an increment of the absolute electronic mean charge, which favors reactivity of the species and, consequently, increases the instability of the absorbance spectra. The found decrease in absorbance in these alkaline conditions (pH = 9.7 and 12.3) is probably due to hydrolysis of riboflavin at high pH values, which is known to cause degradation of the antioxidant following a first-order reaction kinetics.³⁰ For that reason, these pH values are not recommended for the determination of the calibration curve nor for performing extraction.

Because at pH = 8.1 the antioxidant is almost entirely in its neutral stage ($x_{\text{HA}} > 0.97$), as [Table S1](#) shows and as was proved in [Section 3.1](#), and since riboflavin is stable at this pH, as [Figure 3](#) demonstrates, the partition will be performed at

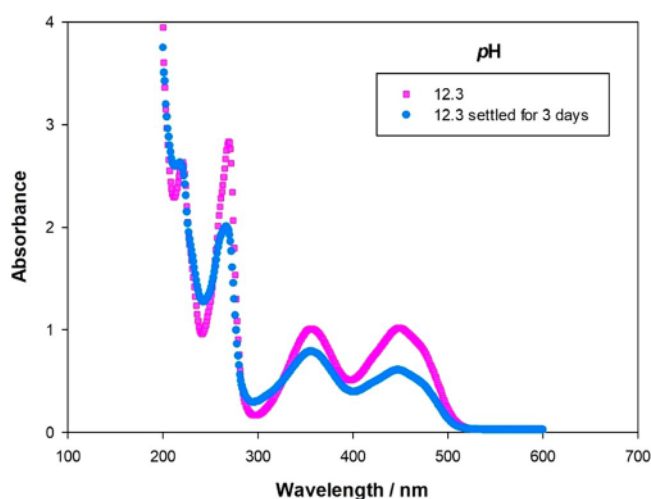


Figure 4. Influence of 3 days of settling on the absorbance spectrum of $5.1 \times 10^{-5} \text{ g} \cdot \text{mL}^{-1}$ of riboflavin in water at pH = 12.3, 298.15 K and 0.1 MPa.

this pH. Therefore, an adequate calibration curve is needed to accurately quantify solute migration to the ATPS phases.

3.3. Absorbance Calibration Curve with Concentrations. To determine the concentration of riboflavin with UV–vis absorbance measurements, the absorbances calibration curve of Figure 5 was obtained, as described in Section 2.4.

The absorbances of pure water (and plate) were subtracted from the experimental results and the curve was determined at 270 nm. At this wavelength, a maximum of absorbance exists and the other ATPS species and pH adjusters do not interfere, as the absorbance spectra of sodium citrate, ethyl lactate, sodium hydroxide and acetic acid (Figures S1–S4) in the Supporting Information, respectively, show.

3.4. Partitioning of Biomolecules. The system {ethyl lactate (1) + sodium citrate (2) + water (3)} was the focus of a previous work,¹³ as Table 2 shows, so there was no need to

study its liquid–liquid equilibria (LLE) and partition in the known tie-lines could be performed straightforwardly.

Table 2. Determined Tie-Lines (TL) for the ATPS {Ethyl Lactate (1) + Nacitrate (2) + Water (3)} at 298.15 K and 0.1 MPa^{a,b,13}

tie-line (TL)	feed		phase	separation		
	w_1/wt	w_2/wt		w_1/wt	w_2/wt	pH
1	30.0	11.0	top	51.7	3.0	7.00
			bottom	16.0	15.7	6.98
2	32.0	11.4	top	57.5	2.0	6.98
			bottom	12.3	18.5	6.96
3	34.3	11.7	top	61.5	1.4	6.98
			bottom	9.8	20.7	6.97
4	36.5	12.1	top	65.0	1.0	7.00
			bottom	7.9	23.0	7.00
5	38.5	12.3	top	67.7	0.7	6.98
			bottom	6.8	24.7	6.97
6	40.6	12.6	top	70.1	0.5	6.98
			bottom	5.5	26.6	7.00

^a w_i stands for the weight percentage (wt %) of species i . ^bStandard uncertainties (u) are $u(T) = 0.2 \text{ K}$, $u(P) = 10 \text{ kPa}$, $u(w_i) = 10^{-1}$, and $u(\text{pH}) = 10^{-2}$.¹³

The partitioning of riboflavin was measured at 298.15 K and 0.1 MPa in the ATPS {ethyl lactate (1) + sodium citrate (2) + water (3)} following the experimental procedure explained in Section 2.5, which implied 6 h of stirring and overnight settling. After separating the phases, mass (m), absorbance (A), pH, and density (ρ) were measured following this order for the top and bottom phases, as Table 3 shows. Moreover, the mass losses (ML) were calculated using

$$\text{ML}/\frac{2-1}{1} \times 100 \quad (10)$$

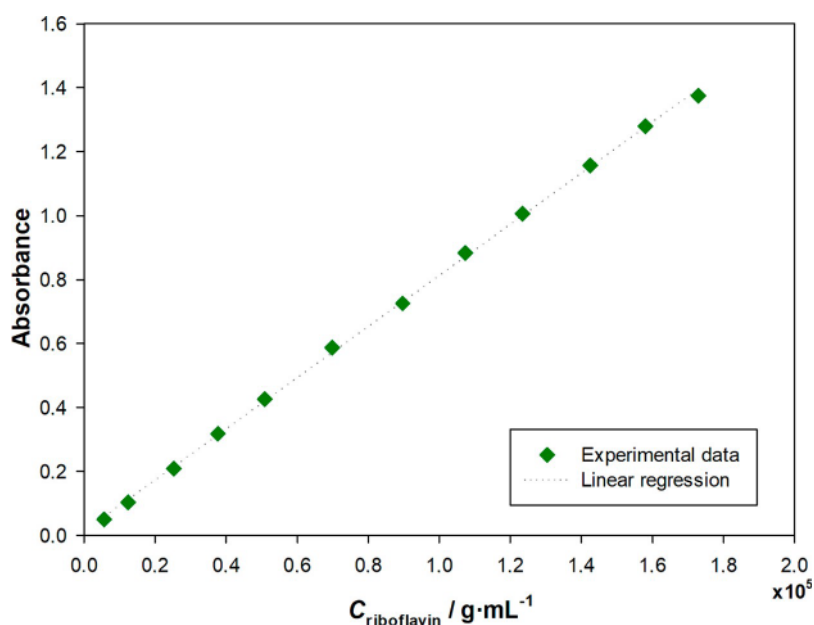


Figure 5. Absorbance calibration curve of riboflavin at 270 nm and pH = 8.1. The first-degree fitting follows equation $A = 80.027 \cdot C \text{ (g} \cdot \text{mL}^{-1}) + 0.0129$ with a correlation coefficient (R) of 0.9997.

Table 3. Experimental Mass (m), Absorbance at 270 nm (A), Density (ρ), pH, and Mass Losses (ML)^a

tie-line (TL)	phase	mass ^b /g	ML ^b	absorbance ^b	density ^b /g·mL ⁻¹	pH ^b
1	top	3.7802	−0.80	1.7448	1.05187	7.591
	bottom	6.2313		0.6514	1.13343	7.447
2	top	4.1057	−0.81	1.8510	1.04713	7.595
	bottom	5.8996		0.5479	1.14750	7.429
3	top	4.6363	−0.64	1.8304	1.04673	7.683
	bottom	5.3569		0.4598	1.16596	7.478
4	top	4.8095	−0.81	1.8560	1.04355	7.853
	bottom	5.1583		0.4063	1.17861	7.426
5	top	4.9922	−0.62	1.8862	1.04324	7.828
	bottom	4.9722		0.3713	1.19151	7.467
6	top	5.2145	−1.37	1.9345	1.04178	7.865
	bottom	4.6192		0.3549	1.20611	7.846

^aFor each phase for the extraction of riboflavin in the ATPS {ethyl lactate (1) + sodium citrate (2) + water (3)} at 298.15 K and 0.1 MPa. ^bThe combined expanded uncertainties (u_c) for a level of confidence of 95% and a combined coverage factor of 1.96³¹ are $u_c(m) = 2 \times 10^{-4}$ g, $u_c(ML) = 0.02$, $u_c(A) = 2 \times 10^{-4}$, $u_c(\rho) = 6 \times 10^{-5}$ g·mL⁻¹, and $u_c(pH) = 0.002$.

where m_1 is the total mass, and m_2 is the sum of masses of the top and bottom phases after separation.

As expected from their relative position, the densities were higher for bottom phases and lower for top phases. Ethyl lactate, which is the extraction solvent, is more abundant in top phases, as seen in Table 2, so these phases have larger antioxidant concentrations and, consequently, bigger absorbances. Concerning pH values, the observed similarity of the top and bottom phases is one of the advantages of using the {ethyl lactate (1) + sodium citrate (2) + water (3)} ATPS. Similar pH values ensure very close mean charges (q) and charged species distribution in the two phases, allowing for comparing absorbances and for using the same calibration curve for top and bottom phases. This way, it is ensured that only the neutral antioxidant stage ($q = 0$ e) is being measured and that the partition coefficients only take in consideration this molecule.

Afterward, the phase volume (V) was determined using eq 11 and riboflavin's concentration (C) was calculated with the absorbances' calibration curve. The difference between the pH of the calibration curve (pH = 8.1) and the pH of the liquid phases (pH ~ 7.6) was disregarded since they correspond to very close fractions of each antioxidant stage (variation of ~1%).

$$V_j = \frac{m_j}{\rho_j} \quad (11)$$

where V_j is the volume, m_j is the measured mass, and ρ_j is the measured density for phase j .

After having determined the concentrations with the calibration curve, the partition coefficients (K) were calculated with eq 12

$$K_i = \frac{C_i^{\text{Top}}}{C_i^{\text{Bottom}}} \quad (12)$$

where C_i^{Top} and C_i^{Bottom} correspond to the riboflavin's concentration in the top and bottom phases, respectively, and i is the tie-line number.

The calculated phase volumes, concentrations and partition coefficients can be observed in Table 4, together with the tie-line lengths reported in a previous work.¹³

In this work, an increasing tie-line number corresponded to larger tie-line lengths (TLL). This result comes from the

Table 4. Calculated Volumes (V) and Antioxidant Concentration (C) for Each Phase, Partition Coefficients (K) for each tie-line and literature-based tie-line lengths (TLL)^a

tie-line (TL)	phase	volume/mL	concentration/g·mL ⁻¹	K	TLL ¹³
1	top	3.5938	1.48×10^{-5}	2.50	37.85
	bottom	5.4977	5.93×10^{-6}		
2	top	3.9209	1.53×10^{-5}	3.04	48.18
	bottom	5.1413	5.04×10^{-6}		
3	top	4.4293	1.52×10^{-5}	3.69	55.17
	bottom	4.5944	4.13×10^{-6}		
4	top	4.6088	1.52×10^{-5}	4.11	61.17
	bottom	4.3766	3.69×10^{-6}		
5	top	4.7853	1.53×10^{-5}	4.89	65.44
	bottom	4.1730	3.12×10^{-6}		
6	top	5.0054	1.57×10^{-5}	6.61	69.68
	bottom	3.8298	2.35×10^{-6}		

^aFor the extraction of riboflavin in the ATPS {ethyl lactate (1) + sodium citrate (2) + water (3)} at 298.15 K and 0.1 MPa.

choosing and numbering of tie-lines and does not convey any important experimental result.

The tie-line with a higher partition coefficient (K) and, therefore, with a more significant difference in antioxidant concentration between the two phases, is tie-line number 6. In the same way, this tie-line also presented the largest tie-line length (TLL), which means that its phases (without antioxidant) were the most distinct composition-wise. To observe this same result, it is common to plot the natural logarithm of K with TLL, which should present a linear relation,¹³ as Figure 6 shows.

Although the linear relation of $\ln(K)$ with the tie-line lengths has not presented a high correlation coefficient, a positive slope was obtained, as expected, and very satisfactory K values were determined, which were significantly larger than the ones reported in literature ($K < 3.5$)²⁷ for the extraction of riboflavin using an ATPS based on PEG and sodium citrate at the same conditions. Therefore, ethyl lactate has a bigger affinity for this antioxidant than polyethylene glycol.

3.5. Mass Balance. In literature, it is common to find partition coefficients (K) based only on the ratio of absorbances. However, not calculating the phase concentration of the solutes nor confirming the validity of the experimental

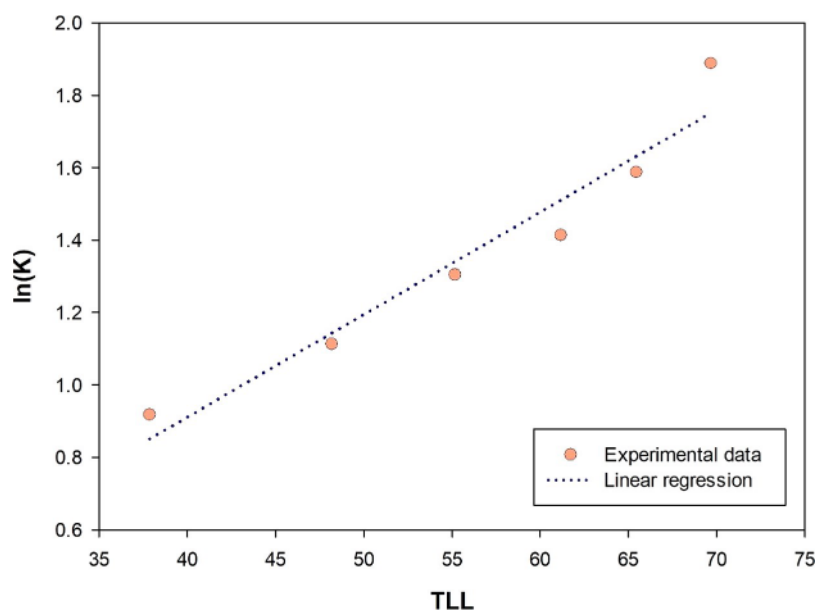


Figure 6. Relation of the tie-line length (TLL)¹³ with the natural logarithm of the partition coefficients (K). The first-degree fitting follows equation $\ln(K) = 0.0283 \cdot \text{TLL} - 0.221$ with a correlation coefficient (R) of 0.9685.

analytical method by checking the mass balance, that is, verifying that all the added solute is being considered by the analytical method, raises questions on some reported conclusions.

The mass balance can be checked by calculating the solute losses (SL), which should be as close as possible to 0 and are calculated using equation

$$\text{SL}/\% = \frac{m_{A2} - m_{A1}}{m_{A1}} \times 100 \quad (13)$$

where m_{A1} is the mass of antioxidant added (present in the 1 mL of stock solution) and m_{A2} is the quantified experimental mass of antioxidant, calculated by

$$m_A = V_i^{\text{Top}} \cdot C_i^{\text{Top}} + V_i^{\text{Bottom}} \cdot C_i^{\text{Bottom}} \quad (14)$$

where V_i^{Top} and V_i^{Bottom} are the calculated experimental volumes of the top and bottom phases, respectively, which are shown in Table 4, and i refers to the tie-line number.

After having calculated the antioxidant masses present in all phases, the extraction efficiencies of each tie-line (E) can be determined using

$$\frac{m_{A2}}{m_{A1}} \times 100 \quad (15)$$

The results can be observed in Table 5, together with the TLL of each tie-line obtained in a previous work.¹³ In the determination of the extraction efficiency ranges, the minimum value was determined using eq 15, whereas for the maximum value $\text{SL} = 0$ was considered.

Table 5 shows that high extraction efficiencies (E) were generally obtained, with tie-line 6 compositions yielding the best result. E increased with growing tie-line length (TLL), following the same behavior as the partition coefficients. On the other hand, very low solute losses were observed (<3), confirming the validity of the analytical method, of the partition coefficients (K) and of the extraction efficiencies (E).

Table 5. Calculated Solute Losses (SL), Extraction Efficiency (E) Range, and Literature-Based TLL^a

tie-line (TL)	SL/%	E range/%	TLL ¹³
1	−1.95	60.9–62.8	37.85
2	−1.21	69.0–70.3	48.18
3	−1.56	76.8–78.4	55.17
4	−1.94	79.7–81.6	61.17
5	−1.74	83.4–85.1	65.44
6	−2.25	87.6–89.9	69.68

^aFor the extraction of riboflavin in the ATPS {ethyl lactate (1) + sodium citrate (2) + water (3)} at 298.15 K and 0.1 MPa.

The extraction efficiencies can be plotted in function of the tie-line lengths, as Figure 7 shows.

As expected, the highest extraction efficiency (E) corresponded to the tie-line with the largest TLL (tie-line

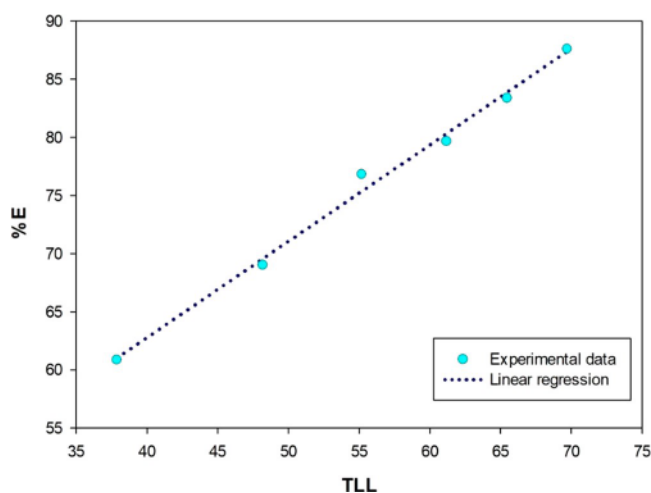


Figure 7. Relation of the TLL¹³ with the extraction efficiencies (E). The first-degree fitting follows equation $E = 1.197 \cdot \text{TLL} - 35.04$ with a correlation coefficient (R) of 0.9967.

number 6), since more distinct compositions ensure bigger differences in polarity and ease partition. A very good linear relation was observed between the extraction efficiencies (E) and TLL, allowing for empirically predicting the E of other tie-line compositions.

4. CONCLUSIONS

The characteristic separation of an ATPS may preclude performing the extraction of biomolecules in their neutral stage or to cause very asymmetrical pH values in the phases. Nevertheless, it is possible to successfully quantify partition if pH is thoroughly studied, since it helps define both a safe extraction for biomolecules (with a pH which ensures stable and known distribution of antioxidant stages) and an accurate analytical method (with adequate wavelength and calibration curves for solute quantification).

The partition of riboflavin (vitamin B2) was successfully performed in the ATPS {ethyl lactate (1) + sodium citrate (2) + water (3)} at 298.15 K and 0.1 MPa. Very high partition coefficients (K) and extraction efficiencies (E) were obtained with the maximum values of 6.61 and 87.6 being observed, respectively, for the longest tie-line (TLL = 69.68). The mass balance was verified, validating the analytical method (UV–vis spectrophotometry) with antioxidant losses below 3%. In conclusion, it was shown that this ATPS can be applied in the purification of riboflavin, which could be promising for future extraction of antioxidants from fruit pomaces.

■ ASSOCIATED CONTENT

SI Supporting Information

The Supporting Information is available free of charge at <https://pubs.acs.org/doi/10.1021/acs.jced.1c00909>.

Absorbance spectra of sodium hydroxide, ethyl lactate, sodium citrate, and acetic acid; absorbance spectra of the stock solutions with different pH values; table with variation of mean charge (q) with pH (PDF)

■ AUTHOR INFORMATION

Corresponding Author

Eugénia A Macedo – LSRE-LCM - Laboratory of Separation and Reaction Engineering – Laboratory of Catalysis and Materials, Faculty of Engineering and ALiCE - Associate Laboratory in Chemical Engineering, Faculty of Engineering, University of Porto, 4200-465 Porto, Portugal; orcid.org/0000-0002-0724-5380; Phone: +351 220 411 653; Email: eamacedo@fe.up.pt

Authors

Pedro Velho – LSRE-LCM - Laboratory of Separation and Reaction Engineering – Laboratory of Catalysis and Materials, Faculty of Engineering and ALiCE - Associate Laboratory in Chemical Engineering, Faculty of Engineering, University of Porto, 4200-465 Porto, Portugal; orcid.org/0000-0003-4802-7301

Ines Oliveira – LSRE-LCM - Laboratory of Separation and Reaction Engineering – Laboratory of Catalysis and Materials, Faculty of Engineering and ALiCE - Associate Laboratory in Chemical Engineering, Faculty of Engineering, University of Porto, 4200-465 Porto, Portugal

Elena Gómez – LSRE-LCM - Laboratory of Separation and Reaction Engineering – Laboratory of Catalysis and Materials, Faculty of Engineering and ALiCE - Associate

Laboratory in Chemical Engineering, Faculty of Engineering, University of Porto, 4200-465 Porto, Portugal

Complete contact information is available at:
<https://pubs.acs.org/doi/10.1021/acs.jced.1c00909>

Notes

The authors declare no competing financial interest.

■ ACKNOWLEDGMENTS

This work was financially supported by LA/P/0045/2020 (ALiCE), UIDB/50020/2020, and UIDP/50020/2020 (LSRE-LCM), funded by national funds through FCT/MCTES (PIDDAC). E.G. thanks funding support from Stimulus of Scientific Employment, Individual Support 2017, CEECIND/02646/2017, FCT.

■ REFERENCES

- (1) Ng, H.; Kee, P.; Yim, H.; Tan, J.; Chow, Y.; Lan, J. Characterization of alcohol/salt aqueous two-phase system for optimal separation of gallic acids. *J. Biosci. Bioeng.* **2021**, *131*, 537–542.
- (2) Albertsson, P. Fractionation of particles and macromolecules in aqueous two-phase systems. *Biochem. Pharmacol.* **1961**, *5*, 351–358.
- (3) Ruiz-Ruiz, F.; Benavides, J.; Aguilar, O.; Rito-Palomares, M. Aqueous two-phase affinity partitioning systems: Current applications and trends. *J. Chromatogr. A* **2012**, *1244*, 1–13.
- (4) McQueen, L.; Lai, D. Ionic Liquid Aqueous Two-Phase Systems From a Pharmaceutical Perspective. *Front. Chem.* **2019**, *7*, 135.
- (5) Suarez Ruiz, C.A.; van den Berg, C.; Wijffels, R.H.; Eppink, M.H.M. Rubisco separation using biocompatible aqueous two-phase systems. *Sep. Purif. Technol.* **2018**, *196*, 254–261.
- (6) Kula, M.; Elling, L.; Walsdorf, A. Investigations of liquid-liquid partition chromatography of proteins. *J. Chromatogr. A* **1991**, *548*, 3–12.
- (7) Iqbal, M.; Tao, Y.; Xie, S.; Zhu, Y.; Chen, D.; Wang, X.; Huang, L.; Peng, D.; Sattar, A.; Shabbir, M.; Hussain, H.; Ahmed, S.; Yuan, Z. Aqueous two-phase system (ATPS): an overview and advances in its applications. *Biol. Proced. Online* **2016**, *18*, 18.
- (8) Schluck, A.; Maurer, G.; Kula, M. Influence of electrostatic interactions on partitioning in aqueous polyethylene glycol/dextran biphasic systems: Part I. *Biotechnol. Bioeng.* **1995**, *46*, 443–451.
- (9) Gomes, G.; Azevedo, A.; Aires-Barros, M.; Prazeres, D. Purification of plasmid DNA with aqueous two phase systems of PEG 600 and sodium citrate/ammonium sulfate. *Sep. Purif. Technol.* **2009**, *65*, 22–30.
- (10) Lu, C.; Gao, L.; Chen, A.; Li, D.; Zhou, Y. The Research and Mechanism of Extracting Vitamin B6 Using Aqueous Two-Phase Systems. *J. Chem.* **2020**, *2020*, 1–12.
- (11) Tanimura, K.; Amau, M.; Kume, R.; Suga, K.; Okamoto, Y.; Umakoshi, H. Characterization of Ionic Liquid Aqueous Two-Phase Systems: Phase Separation Behaviors and the Hydrophobicity Index between the Two Phases. *J. Phys. Chem. B* **2019**, *123*, 5866–5874.
- (12) Ooi, C.; Tey, B.; Hii, S.; Kamal, S.; Lan, J.; Ariff, A.; Ling, T. Purification of lipase derived from *Burkholderia pseudomallei* with alcohol/salt-based aqueous two-phase systems. *Process Biochem.* **2009**, *44*, 1083–1087.
- (13) Velho, P.; Requejo, P.; Gómez, E.; Macedo, E. A. Novel ethyl lactate based ATPS for the purification of rutin and quercetin. *Sep. Purif. Technol.* **2020**, *252*, 117447.
- (14) Pereira, C.; Silva, V.; Rodrigues, A. Ethyl lactate as a solvent: Properties, applications and production processes – a review. *Green Chem.* **2011**, *13*, 2658.
- (15) Requejo, P.; Velho, P.; Gómez, E.; Macedo, E. A. Study of Liquid–Liquid Equilibrium of Aqueous Two-Phase Systems Based on Ethyl Lactate and Partitioning of Rutin and Quercetin. *Ind. Eng. Chem. Res.* **2020**, *59*, 21196–21204.

- (16) Velho, P.; Requejo, P.; Gómez, E.; Macedo, E. A. Thermodynamic study of ATPS involving ethyl lactate and different inorganic salts. *Sep. Purif. Technol.* **2021**, *275*, 119155.
- (17) Liu, S. Woody biomass: Niche position as a source of sustainable renewable chemicals and energy and kinetics of hot-water extraction/hydrolysis. *Biotechnol. Adv.* **2010**, *28*, 563–582.
- (18) Panzella, L.; Moccia, F.; Toscanesi, M.; Trifuoggi, M.; Giovando, S.; Napolitano, A. Exhausted Woods from Tannin Extraction as an Unexplored Waste Biomass: Evaluation of the Antioxidant and Pollutant Adsorption Properties and Activating Effects of Hydrolytic Treatments. *Antioxidants* **2019**, *8*, 84.
- (19) Posadino, A.; Cossu, A.; Giordo, R.; Piscopo, A.; Abdel-Rahman, W.; Piga, A.; Pintus, G. Antioxidant Properties of Olive Mill Wastewater Polyphenolic Extracts on Human Endothelial and Vascular Smooth Muscle Cells. *Foods* **2021**, *10*, 800.
- (20) Krivokapic, S.đ.; Vlaovic, M.; Damjanovic Vratnica, B.; Perovic, A.; Perovic, S. Biowaste as a Potential Source of Bioactive Compounds - A Case Study of Raspberry Fruit Pomace. *Foods* **2021**, *10*, 706.
- (21) Henriksen, E. Role of Oxidative Stress in the Pathogenesis of Insulin Resistance and Type 2 Diabetes. *Bioact. Food Diet. Interventions Diabetes* **2019**, 3–17.
- (22) Mathew, M.; Ervin, A.; Tao, J.; Davis, R.; Antioxidant vitamin supplementation for preventing and slowing the progression of age-related cataract. *Cochrane Database Syst. Rev.*; Wiley, 2012..
- (23) Amevor, F.; Cui, Z.; Ning, Z.; Du, X.; Jin, N.; Shu, G.; Deng, X.; Zhu, Q.; Tian, Y.; Li, D.; Wang, Y.; Zhang, Z.; Zhao, X. Synergistic effects of quercetin and vitamin E on egg production, egg quality, and immunity in aging breeder hens. *Poult. Sci.* **2021**, *100*, 101481.
- (24) Gibb, Z.; Blanco-Prieto, O.; Bucci, D. The role of endogenous antioxidants in male animal fertility. *Res. Vet. Sci.* **2021**, *136*, 495–502.
- (25) Masaki, H. Role of antioxidants in the skin: Anti-aging effects. *J. Dermatol. Sci.* **2010**, *58*, 85–90.
- (26) Saedisomeolia, A.; Ashoori, M. Riboflavin in Human Health: A Review of Current Evidences. *Adv. Food Nutr. Res.* **2018**, *83*, 57–81.
- (27) Wysoczanska, K.; Do, H. T.; Sadowski, G.; Macedo, E. A.; Held, C. Partitioning of water-soluble vitamins in biodegradable aqueous two-phase systems: Electrolyte perturbed-chain statistical associating fluid theory predictions and experimental validation. *AIChE J.* **2020**, *66*, e16984.
- (28) Brittain, H. *Profiles of drug substances, excipients and related methodology: critical compilation of pKa values for pharmaceutical substances*; Elsevier, 2007; p 33.
- (29) Zhou, T.; Jhamb, S.; Liang, X.; Sundmacher, K.; Gani, R. Prediction of acid dissociation constants of organic compounds using group contribution methods. *Chem. Eng. Sci.* **2018**, *183*, 95–105.
- (30) Surrey, A.; Nachod, F. Alkaline Hydrolysis of Riboflavin. *J. Am. Chem. Soc.* **1951**, *73*, 2336–2338.
- (31) Chirico, R. D.; Frenkel, M.; Diky, V. V.; Marsh, K. N.; Wilhoit, R. C. ThermoMLAn XML-Based Approach for Storage and Exchange of Experimental and Critically Evaluated Thermophysical and Thermochemical Property Data. 2. Uncertainties. *J. Chem. Eng. Data* **2003**, *48*, 1344–1359.

Recommended by ACS

Densities, Viscosities, and Derived Properties for Binary Mixtures of Long-Chain Alcohols of 1-Hexanol + 1-Pentanol, + 2-Pentanol, + 2-Methyl-1-butanol, + 1-Heptanol, and +...

José J. Cano-Gómez, Mónica M. Alcalá-Rodríguez, *et al.*

MARCH 03, 2023

JOURNAL OF CHEMICAL & ENGINEERING DATA

READ 

Selective Extraction of Antioxidants by Formation of a Deep Eutectic Mixture through Mechanical Mixing

Idrees B. Qader, Andrew P. Abbott, *et al.*

FEBRUARY 27, 2023

ACS SUSTAINABLE CHEMISTRY & ENGINEERING

READ 

Density Functional Theory Study of the Molecular Interaction between Selective Phenolic Compounds and Glycerol-Based Deep Eutectic Solvents

Vichitra Malaiyarasan, Sujatha Ramalingam, *et al.*

DECEMBER 14, 2022

ACS AGRICULTURAL SCIENCE & TECHNOLOGY

READ 

Estimating Water Solubilities of Monofunctional, Uncharged Organic Molecules

Timothy S. Eckert.

MARCH 03, 2023

JOURNAL OF CHEMICAL EDUCATION

READ 

Get More Suggestions >